NJC

New Journal of Chemistry

A journal for new directions in chemistry

Accepted Manuscript

This article can be cited before page numbers have been issued, to do this please use: E. Diguilio, E. Galarza, M. E. Domine, L. Pierella and M. S. Renzini, *New J. Chem.*, 2020, DOI: 10.1039/C9NJ04106K.

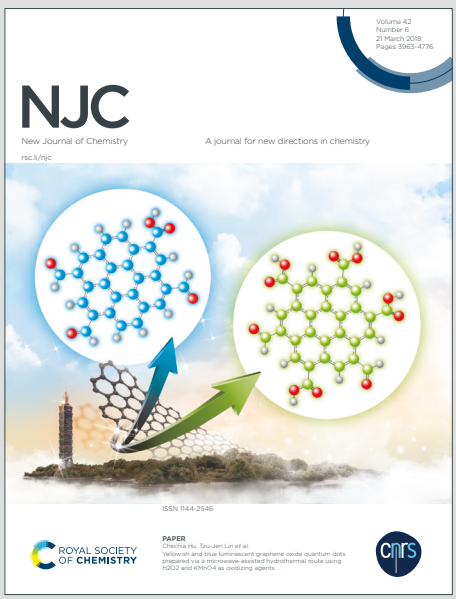

This is an Accepted Manuscript, which has been through the Royal Society of Chemistry peer review process and has been accepted for publication.

Accepted Manuscripts are published online shortly after acceptance, before technical editing, formatting and proof reading. Using this free service, authors can make their results available to the community, in citable form, before we publish the edited article. We will replace this Accepted Manuscript with the edited and formatted Advance Article as soon as it is available.

You can find more information about Accepted Manuscripts in the Information for Authors.

Please note that technical editing may introduce minor changes to the text and/or graphics, which may alter content. The journal's standard Terms & Conditions and the Ethical guidelines still apply. In no event shall the Royal Society of Chemistry be held responsible for any errors or omissions in this Accepted Manuscript or any consequences arising from the use of any information it contains.

Tuning products selectivity in the catalytic oxidation of glycerol employing Metal-ZSM-11 materials

Diguilio, Eliana[1]; Galarza, Emilce D.[1]; Domine, Marcelo E.[2]; Pierella, Liliana B.[1] and Renzini, María S.[1]

[1]Centro de Investigación y Tecnología Química (CITeQ), UE CONICET- Universidad Tecnológica Nacional, Facultad Regional Córdoba, Maestro Lopez esq Cruz Roja Argentina, Ciudad Universitaria, (5016) Córdoba, Argentina. E-mail: ediguilio@frc.utn.edu.ar

2 Instituto de Tecnología Química (UPV-CSIC), Universitat Politècnica de València, Consejo Superior de Investigaciones Científicas, Avda. de los Naranjos s/n, 46022, Valencia, España.

Abstract.

Copper and chromium supported on ZSM-11 (MEL type structure) microporous zeolites were investigated as catalysts for glycerol oxidation towards dihydroxyacetone and lactic acid. ZSM-11 was synthesized by hydrothermal crystallization. Subsequently an alkaline treatment of desilication was carried out, in order to generate zeolites with micro-mesoporosity. An ionic exchange with ammonium chloride was done to recover acids sites, and then, Cr (III) and Cu (II) species were incorporated onto these materials. Finally, thermal treatment at 500 ºC was carried out. These materials were characterized by different techniques, and then, evaluated in glycerol oxidation reaction, employing H_2O_2 as an oxidizing agent. The maximum conversion of glycerol (≈70%) was reached over Cr-ZSM-11 catalyst, with selectivity to dihydroxyacetone of ≈28%. Meanwhile Cu-ZSM-11 offered 50% of glycerol conversion with selectivity to 68% towards lactic acid. In both cases, the optimal reaction conditions were studied to maximize the selectivity towards the products above-mentioned.

Key Words. Glycerol Oxidation, Cu, Cr-Zeolites; Dihydroxyacetone, Lactic Acid. DOI: 10.1039/C9NJ04106K

1. Introduction

In recent years, biodiesel industry has increased its production worldwide, mainly due to the decline in fossil fuel reserves with the consequent increase in the price of oil. Biodiesel is synthesized via the transesterification of triglycerides (vegetable oils) with methanol to produce the corresponding fatty acid methyl esters (FAMEs). The raw materials commonly employed as source of triglycerides used to be colza, sunflower, soybean and palm oil, among other, and the biodiesel obtained can be applied directly as fuel or blended with petroleum-derived diesel fractions in different ratios [1].

USA, Brazil, Argentina, Indonesia, and Malaysia are between the top biodiesel producer countries in the world, followed by others such as Thailand, Uruguay, and Colombia. Exterior Agriculture Service (USDA, Bs. As.) of Argentina has reported national production of biodiesel in 2018 in more than 2, 0 million of tons, close to the production of 2, 3 million tons generated in 2017, and 2, 6 million tons in 2016, which was the record year. Exports of biodiesel remained unchanged in 2018 compared to the previous year (1, 4 million of tons/year), while domestic consumption decreased in ≈ 22%.

The main by-product in biodiesel production is glycerol (10% in weight of total production). The exportation of crude glycerol in December 2018, has diminish in 25,4 % respect to December 2017, with a decrease in its price due to the high supply in the market according was informed by the Argentina Biofuel Camera (Report 2018, 2019)[2] . Therefore, in recent years, the interest in find alternatives to increase the productivity of the biodiesel chain has arisen, generating added value to the main by-product. Moreover, glycerol accumulation in biodiesel plants can cause environmental problems, becoming into an inconvenient waste.

View Article Online
DOI: 10.1039/C9NJ04106K

Glycerol (GLY) is a useful chemical with many industrial applications such as cosmetics (soaps, creams), lubricants, paints and food industry, as well as intermediate in the production of synthetic fibers. It is considered as one of the most important building block molecules derived from biomass, from which can be obtained a large variety of higher value-added compounds [3].

In recent years, numerous glycerol valorization routes have been studied. One of the most important and non-commercialized routes for glycerol valorization is the selective oxidation of glycerol (GLY) in liquid phase. In this process, a large number of products are generated mainly due to the high functionality of glycerol molecule. One of these products is dihydroxyacetone (DHA), a simple carbohydrate with highest commercial value due to its use in pharmaceutical and cosmetic industry. Other products from glycerol oxidation are glyceraldehyde (GLYALD), as well as glyceric (GLYAC), glycolic (GLYCAC), lactic acid (LA) and hydroxy-pyruvic (HYPAC) acids; most of these compounds result interesting for applications in cosmetic, plastic and pharmaceutical industries [4 56].

This work is focused on the production of DHA and LA from glycerol, since both are relevant chemicals for several industries.

On one hand, DHA is a carbohydrate with three carbon atoms, widely used in cosmetic industry to produce sunscreens. In addition, DHA combined with pyruvate results in an effective nutritional supplement than can help to eliminate fat and increase muscle mass[7]. Nowadays, DHA is produced from the microbial fermentation of glycerol employing Gluconobacter oxidans with 87-94% yield after ~32 h. The productivity to DHA is relatively low due to the low glycerol concentration in aqueous solution and the long reaction times applied [89].The direct catalytic oxidation of glycerol to DHA over Au, Pt and Pd supported catalysts has been studied a few years ago. Nevertheless, the use of

these metals results expensive and has some drawbacks such as the catalyst deactivation, mainly due to the sintering of metal nano-particles and the leaching of metals in the reaction medium [1011]. In this sense, it is of great interest the design of heterogeneous catalysts possessing transition metals, with low cost and high resistance under reaction conditions that also result efficient and selective towards the desired product [12].

Hu et al. have investigated glycerol selective oxidation to dihydroxyacetone in a semi-batch reactor over Pt-Bi/C catalyst, with a maximum DHA yield reported of 48% at 80% glycerol conversion [13]. Recently, Crotti et al. have tested an "in situ" prepared iron complex [Fe $(BPA)_2(OTf)_2$] as alcohol oxidation catalyst, employing H_2O/CH_3CN as reaction medium, and obtaining DHA selectivity of 53% after 90 min. of reaction at 25 °C [14]. Other authors have studied a series of sulfonato-salen metal complexes intercalated into Mg-Al layer double hydroxide (LDH) with transition metals for the selective oxidation of glycerol to produce dihydroxyacetone (DHA). The glycerol conversion was 40.3% and DHA selectivity reached 52.9% over Cu(II) sulfonato-salen-intercalated LDH catalyst (at 60 °C, during 4 h and pH = 7), while glycerol conversion was 57.0% employing Cr(III) sulfonate-salen-intercalated LDH catalyst and DHA selectivity was 42.3% under similar reaction conditions [14].

On the other hand, LA (2-hydroxypropanoic acid or lactic acid) is an organic acid widely distributed in nature, which is actually being a molecule of great interest in the booming bio-refinery industry. Due to its different properties [15], lactic acid is an important industrial product with several applications as food additive, as well as in cosmetics and pharmaceuticals. Currently, more attention has been paid on the potential use of LA as monomer in the production of a biodegradable poly-lactic acid or polylactide, thermoplastic aliphatic polyester with a wide range of applications in the polymer industry. Li et al. have investigated Ni promoted noble metal catalysts for the glycerol

View Article Online
DOI: 10.1039/C9NJ04106K

oxidation to LA in the presence of NaOH solution, achieving practically 100% glycerol conversion and 62.6% LA selectivity in the first run of the reaction. However, the glycerol conversion declined from ≈100% to 57.2% during the recycling experiments [16]. In addition, Zhang et al. [17] have studied the use of a series of copper-promoted platinum supported on activated carbon (Cu-Pt/AC) catalysts for glycerol oxidation to lactic acid. At 90°C, the average glycerol conversions were 56% with selectivity to LA lower than 72%.

Considering the scarcity and price of noble metals, exploring and developing novel, efficient, and resistant catalysts with lower cost (by using non-noble metals) is highly desirable. Following this idea, here is proposed the study of the catalytic oxidation of GLY using modified ZSM-11 zeolites by alkaline treatment, generating a combined micro-mesoporosity system. Each porosity in the hierarchical structure exhibits differences, while microporous hold catalytically active sites, the access to the pores is facilitated by mesoporous. Hierarchical zeolites exhibits improved accessibility to the active sites, which facilitates mass transport of molecules, and they result more resistant to deactivation by coke formation. Consequently, these materials show a higher catalytic activity than conventional zeolites, in particular in those reactions that include bulky molecules because prevent diffusional limitations. Furthermore, the secondary porosity allows greater access to the active phases (cations, metal oxides, metal salts and metal complexes) located in the external surface or micropores of the zeolites [418]. Subsequently the synthesized micro/mesoporous materials will be impregnated with transition metals of Copper (II) and Chromium (III), to be evaluated as catalysts in the oxidation of glycerol in liquid phase.

The optimal reaction conditions are properly studied and discussed in the following sections. The adequate selection of metal and its presence in the tailor-made ZSM-11

zeolite structure allow us tuning catalyst properties and driving reaction mechanism to the attainment of dihydroxyacetone (DHA) or lactic acid (LA) desired products.

2. Experimental

2.1 Catalysts preparation

ZSM-11 zeolite was synthetized by hydrothermal crystallization, at 140 ºC, using tetrabutyl ammonium hydroxide (TBAOH) as a structure-directing agent [19]. The obtained gel was extracted by filtration, washed with deionized water, and then dried at 100 °C during 24 h. To remove TBAOH, a thermal treatment was carried out in N_2 atmosphere (20 ml/min) at programmed temperature (20° C/min) from ambient temperature up to 500 °C. Then, the solid was calcined in static air at 500 °C during 8 h to obtain the Na-ZSM-11 material. NH_4-ZSM-11 form of the zeolite was prepared by ion exchange of the as-prepared Na-zeolite with 1 M ammonium chloride aqueous solution at 80 °C during 40 h. Finally, thermal treatment (calcination) at 500 ºC under a N_2 stream was applied to the NH_4-zeolite to finally obtain the protonic form of the H-ZSM-11 zeolite.

2.1.1 Alkaline post-synthesis treatment

The generation of mesoporous in microporous zeolites was carried out by post-synthesis desilication treatment [20]. The methodology consisted in the hydrolysis of the Si-O-Si bonds by reacting the microporous zeolite with an alkaline solution of NaOH. This procedure allows the generation of mesoporosity while the acidic properties of the zeolite were maintained. For this purpose, 1 g of Na-ZSM-11 was placed in a flask and treated with 30 ml of NaOH aqueous solution (0.3 M). The system was immersed in a water bath with constant magnetic stirring to maintain a constant temperature of 65 °C during 30 min. After reaction, the solid material was recovered by filtration, and then dried at 100 °C overnight. Finally, three successive exchanges were performed employing NH_4Cl aqueous solution (0.5 M) at 80 °C during 1 h. The solid was again filtered under vacuum,

and dried at 100 °C during 12 h. Thermal treatment (calcination) at 500 ºC under a N_2 stream was carried out to remove residual salts, thus obtaining the NH_4-ZSM-11 (T) material. Later on, this material will be modified by incorporation of transition metals.

2.1.2 Incorporation of transition metals

Synthesized zeolites were modified by introduction of transition metals such as Cr (III) and Cu (II). These metals were incorporated to the NH_4-zeolite form by wet impregnation method. To this purpose, the catalyst was suspended in aqueous solution of the corresponding metal precursor, $Cl_3Cr.6H_2O$ (Fluka, 98%) for Cr-zeolite and Cu $(C_2H_3O_2)_2.H_2O$ (Mallinckrodt, ACS) for Cu-zeolite. Then, the samples were evaporated at 80 °C under vacuum, until complete dryness. After that, the solids were dried at 100 °C in an oven during 24 h. Finally, Cr-zeolite and Cu- zeolite were thermally treated under N_2 flow (20 ml/ min) from ambient temperature up to 500 °C, with a heating ramp of 20°C/min, during 8 h, followed by calcination in static air under the same conditions.

2.2 Catalysts Characterization

Catalytic materials were characterized by different techniques:

- X-ray diffraction (XRD) was employed to determine the structure and the crystallinity level of the zeolitic materials, by using a Philips PW 3020 diffractometer using CuKα radiation. Diffraction data were recorded from 2θ = 2º - 60º at an interval of 0.1º and scanning speed of 2 º/min was used. Relative crystallinity of the zeolitic materials was calculated by using the following formula (where Pattern refers to a standard sample of ZSM-11 zeolite synthesized in our research group) [21].

$$\%\ Crystallinity = \frac{Area\ under\ the\ peaks\ shows\ X}{Area\ under\ the\ peaks\ shows\ Pattern} * 100$$

Infrared spectroscopy analysis were performed in a JASCO 5300 FTIR spectrometer.

For the structural characterization in the lattice vibration region (400−1800 cm^{-1}), the samples were mixed with KBr at 0.05% and pressed to form wafers. To determine the type and concentration of acidic sites, pyridine (probe molecule) adsorption experiments were carried out on self-supporting wafers (10−20 mg/cm^2) of the zeolites, using a thermostatted cell with CaF_2 windows connected to a vacuum line.

Pyridine (3 Torr) was adsorbed at room temperature and desorbed (10^{-4} Torr) at 250, 350, and 400 °C during 1 h. Finally, the number of Brønsted and Lewis acid sites was calculated from the maximum intensity of the adsorption bands (1545 and 1450−1460 cm^{-1}, respectively). These values were calculated by using literature data of the integrated molar extinction coefficients, which are independent of the catalysts or strength of the sites [22].

- BET surface area determinations were carried out with ASAP 2000 equipment with N_2 absorption at 77 K.

- Nitrogen sorption isotherms were measured in Micromeritics apparatus Model ASAP 2010 equipment. It was determined the total pore volume of zeolites at relative gas pressure (p/p_0) = 0.98, assuming complete filling of pores. Micropore volume (V_{micro}) was determined by t-plot method. Mesopore volume was calculated by difference between total and micropore volume ($V_{Total} - V_{micro} = V_{meso}$).

- The metal content and Si/Al relation in the zeolites were determined by an inductively coupled plasma-atomic emission spectrometer ICP Varian 715ES.

- UV–Vis-DR spectra of the materials were recorded using a Perkin Elmer precisely – Lambda 35 spectrophotometer, to which a diffuse reflectance chamber Labsphere RSA-PE-20 with an integrating sphere of 50 mm diameter and internal Spectralon coating is attached.

- Transmission electron microscopy measurements were performed on JEM 2010 Plus electron microscope, equipped with EDS Oxford X-MAX 65 T operating at 200 kv. The samples were pre-treated by ultrasonic dispersion in ethanol, and then dropped onto grids.

2.3 Catalytic experiments

The catalytic activity of the metal-zeolites here prepared was evaluated in the selective oxidation of GLY (Merck, ACS reagent) in liquid phase. The reaction was carried out in a glass reactor (25 ml) with two necks, and equipped with a condenser and a magnetic stirrer. The system was submerged in a water bath that allowed maintaining a constant temperature (60 °C) all along the experiment. An aqueous solution of GLY (0.5 M) was placed in the reactor, with H_2O_2 as oxidizing agent (30% v/v) and 200 mg of catalyst. The reaction products were identified and quantified by liquid chromatography (HPLC), in a Jasco UV-975/ PU-980. An Aminex HPX - 87H column set at 50 °C, a UV-VIS detector (210 nm) and a Refractive Index detector coupled in series were employed. The mobile phase was sulfuric acid (5mM) at 0.6 ml/min. The identification and quantification of the oxidation products was done by comparison with the pure standards using calibration curves.

The optimal reaction conditions were studied in this work employing the Cr-ZSM-11 and Cu-ZSM-11 zeolites as catalysts, with the aim to obtain the maximum selectivity to DHA and LA, respectively. The reaction temperature was varied in a range of 60 to 80 °C, reaction times from 60 a 240 min, and the amount of catalyst from 0.1 to 0.3 g, whereas the substrate/H_2O_2 molar ratio (R) was also studied (R = 0.3 - 0.5 - 075 - 1).

In some cases, the efficiency of H_2O_2 (mols of oxidating agent that are consumed to transform GLY in oxydated products) was calculated by means of iodometric titration employing sodium thiosulfate as titrant solution. This H_2O_2 efficiency (*Eff* H_2O_2) was obtained as a percentage by applying the following equation:

View Article Online
DOI: 10.1039/C9NJ04106K

$$Eff\ H2O2 = \frac{moles\ converted}{moles\ consumed}\ x\ 100$$

Finally, the reuse and recyclability of the catalysts (Cr-ZSM-11 and Cu-ZSM-11) was evaluated. For that, the used solid catalyst was recovered from the reaction mixture by filtration, and then washed with water. Afterwards, the catalyst was used in a new experiment without any regeneration treatment.

3. Results and Discussion

3.1 Catalysts characterization

X-ray diffraction patterns of Cr-Zeolites and Cu-Zeolites obtained by incorporation of transition metals in both conventional and post-treated (T) ZSM-11 zeolites are shown in Figure 1. As can be seen, all of the as-obtained solids showed the presence of a highly crystalline MEL-type zeolitic structure with well-defined diffraction peaks of a high structural order (2θ = 7-8° and 2θ = 21-22°). XRD patterns clearly show that zeolitic structures were not influenced by the incorporation of transition metals using the impregnation method. For Cr-zeolites, the characteristic peaks of the chromium oxide Cr_2O_3 (*) were observed, which is an evidence of the presence of Cr^{+3} species in the zeolite. In the case of the Cu-Zeolite samples, no characteristic CuO signals are observed, which could be an indication that the Cu has been almost completely exchanged, the percentage of metal deposited as oxide being very low (not detectable by XRD).

View Article Online
DOI: 10.1039/C9NJ04106K

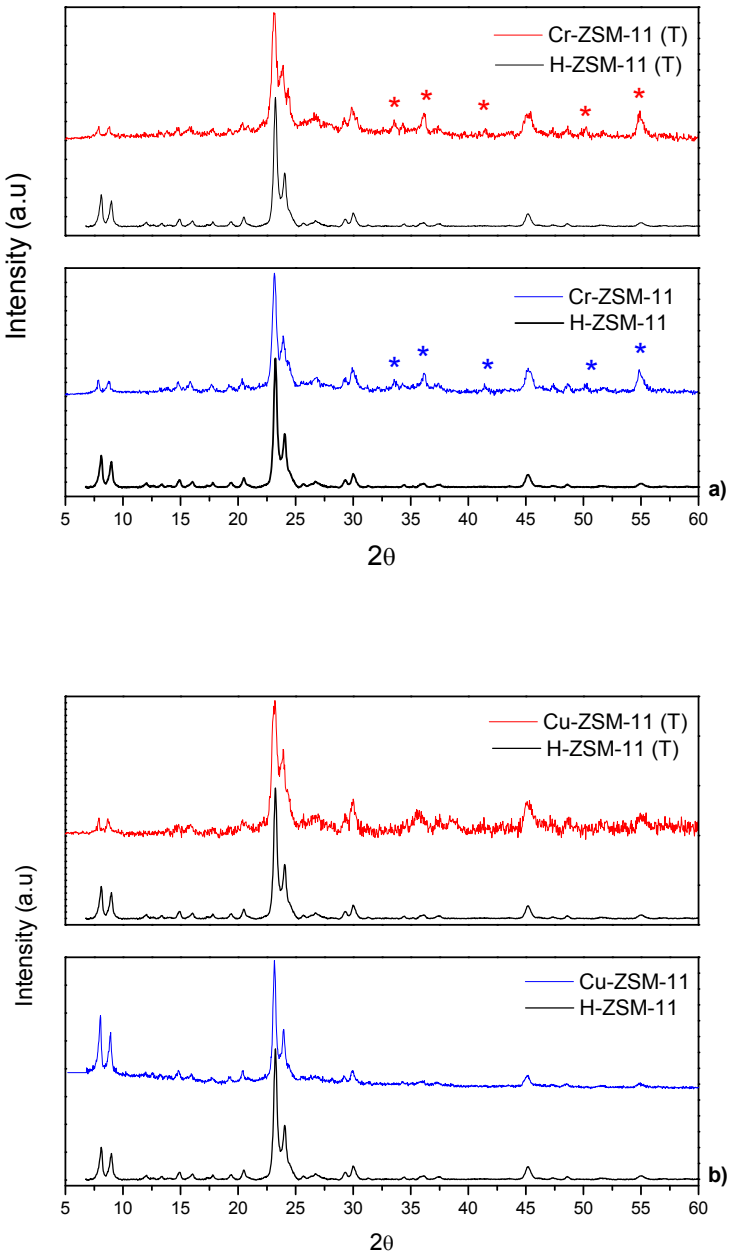

Figure 1. XRD patterns of a) Cr-ZSM-11 and Cr-ZSM-11 (T), b) Cu-ZSM-11 and Cu-ZSM-11 (T).

The main physicochemical and textural properties of the zeolites measured by different techniques such as ICP, N_2 sorption isotherms; XRD and FTIR are summarized in Table 1. The content of metal effectively incorporated in the zeolites was very close to the theoretical calculated values. Surface area determined by means of BET method of the conventional ZSM-11 was around of 390 m^2/g, while it was slightly increased in the

micro-mesoporous ZSM-11 (T). The relative crystallinity was higher than 97-99% in all cases, which indicates that the crystalline structure of the zeolites is maintained with high purity after both the chemical and thermal treatments.

Table 1. Main physicochemical and textural properties of the catalysts.

Catalysts	Si/Al molar ratio	Cu, Cr (wt. %)	Surface area (m^2/g)	Relative Crystallinity (%)		B/L[c]
	ICP	ICP	BET[a]	XRD	FTIR[b]	FTIR
H-ZSM-11	18.02	-	390	100	>99	9.20
H-ZSM-11 (T)	15.59	-	430	>97	>97	1.56
Cu-ZSM-11	18.04	3.11	392	100	>99	0.64
Cu-ZSM-11 (T)	16.72	2.90	430	>97	>97	0.08
Cr-ZSM-11	18.01	2.98	390	100	>99	2.96
Cr-ZSM-11 (T)	17.91	2.99	433	>97	>97	0.79

[a] Surface area values calculated from N_2 sorption isotherms by means of BET method.
[b] FTIR in the fingerprint zone of the materials (400−1200 cm^{-1}).
[c] Lewis acid sites (µmol Py/g of catalyst) and Lewis/Brønsted sites ratio obtained from FTIR spectra of pyridine absorbed at room temperature and desorbed at 400°C.

The textural properties of these materials before and after desilication treatment were obtained by N_2 sorption isotherms at -196 °C. On one hand, the isotherms of the synthesized zeolites were isotherms type I (see Supporting Information Figure S1), characteristics of microporous structures according to the IUPAC classification. On the other hand, the hierarchical zeolites, obtained after desilication treatment, exhibit isotherms combining type I-IV, with greater adsorption at P/P_0 between 0.4-1.0, this indicating the existence of voids between particles with irregular shape with broad size distribution [23].

The total Pore Volume (cm^3/g) is high in zeolites with alkaline treatment (Cr- and Cu-ZSM-11 (T)), which is directly related to the increase of mesopore volume and the small decrease in micropore volume; all these observations clearly indicate the generation of mesoporosity in these materials. Determination of the pore size distribution by following

BJH method was also possible, the obtained values being between 2 and 10 nm (Supporting Information Figure S2).

The FTIR spectra of pyridine adsorbed on conventional and hierarchical metal-zeolites are depicted in Figure 2, only showing the wavelength zone from 1400 to 1700 cm^{-1}.

In Table 1 it is shown the Brønsted to Lewis acid sites ratio of the zeolites calculated from FTIR spectra of pyridine absorbed at room temperature and desorbed at 400°C.

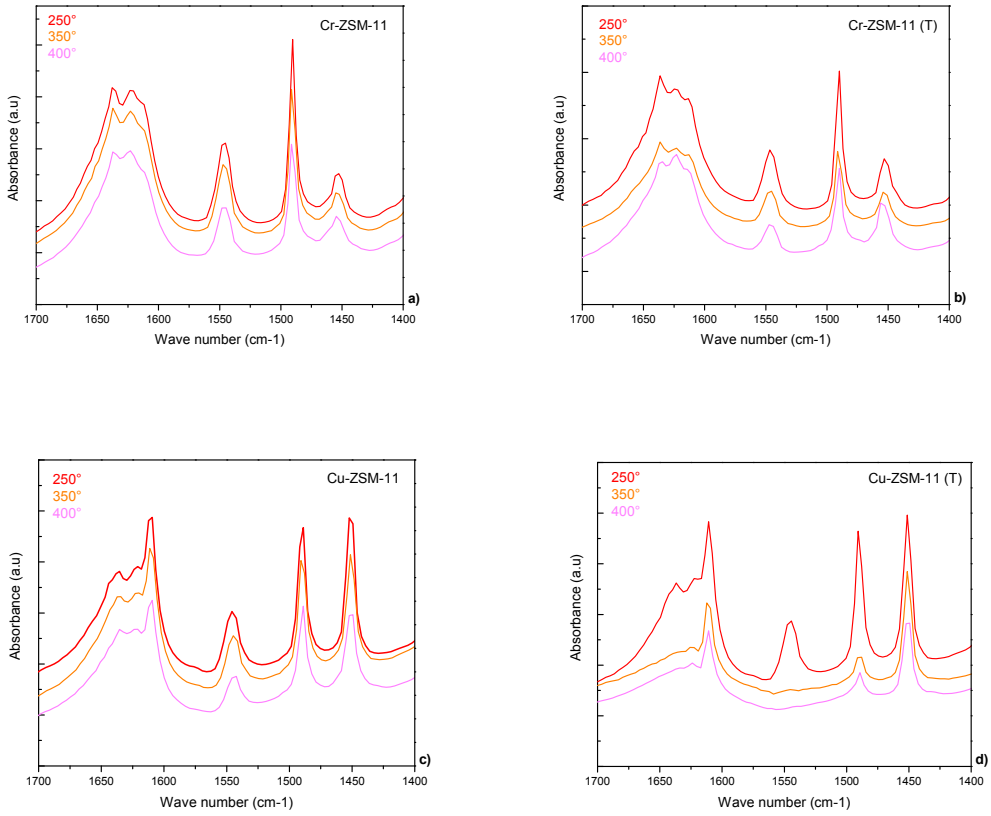

Figure 2. FTIR spectra of pyridine absorption experiments at room temperature and desorption at 250, 350 and 400ºC, a) Cr-ZSM-11, b) Cr-ZSM-11 (T), c) Cu-ZSM-11 and d) Cu-ZSM-11 (T).

The band at 1638 cm^{-1}, which is assigned to structural OH^- ion vibration, is indicative of the interaction of pyridine with Brønsted acid sites (PyH^+). Bands at wavenumbers 1620−1623 cm^{-1} would result from strong Lewis sites, whereas bands at lower wavenumbers (1614 cm^{-1}) would indicate medium to strong sites. Interestingly, the

View Article Online
DOI: 10.1039/C9NJ04106K

intensity of these bands was greatly affected by desilication treatment, especially in Cu-ZSM-11 (T), due to a great dissolution of Si-OH groups. The band at 1490 cm^{-1} corresponds to the vibration of pyridine adsorbed over Brønsted and Lewis acid sites. The band at 1455 cm^{-1} corresponds to the interaction of pyridine with Lewis acid sites (PyL), and the band at 1545 cm^{-1} is indicative of the interaction of pyridine with Brønsted acid sites (PyH^+). It can be observed that the intensity of this band decreases in metal-zeolites after alkaline treatment, until total disappearance in Cu-ZSM-11 (T) [24]. Upon metal cation introduction, the Lewis acid sites were significantly increased in both metal- zeolites (Cr, Cu) with respect to H-ZSM-11 catalyst, resulting in a higher ratio of acid sites Lewis to Brønsted mostly in Cu-ZSM-11 (T).

In literature it was proposed that in desilicated zeolites the majority of Lewis sites are created from dehydroxylation of the Si–OH–Al groups, after the reinsertion of some Al extracted during alkaline treatment. Consequently, the new Lewis sites formed are primarily located on the mesopore surfaces, allowing accessibility of larger molecules. Some Al may remain in extra- framework positions, modifying the acidity of these materials. Some catalytic application may require an Al species extra-framework such as Lewis acid centers or a reduced concentration of Brønsted acid sites. These reactions generally are benefited by micro-mesoporosity for improved transport of molecules [18,25].

The morphology, distribution and the particle size of metal-based catalysts were determined by Transmission electron microscopy (TEM) measurements. TEM images of the samples are presented in Figures 3 and 4, where the dark spots of the images would be the particles of Cu and Cr that have been incorporated in the zeolite ZSM-11 by wet impregnation. In order to investigate the dispersion and average size of the particles, the TEM micrograph was analysed by using Image J NIH program, thus counting more than 50 metal nanoparticles in each case. In this way the particle size distribution of the

View Article Online
DOI: 10.1039/C9NJ04106K

samples was obtained too. The application of the procedure above mentioned resulted in Cu nanoparticle sizes between 0.5 and 3.5 nm, with greater distribution between 1.0 and 2.5 nm, with an average size of 1.8 nm, showing a heterogeneous dispersion of the crystals on the solid surface. Small particle size favours that metal nanoparticles have a greater area exposed to the reactant molecules, thus increasing the catalytic activity of this material in the conversion of GLY [17].

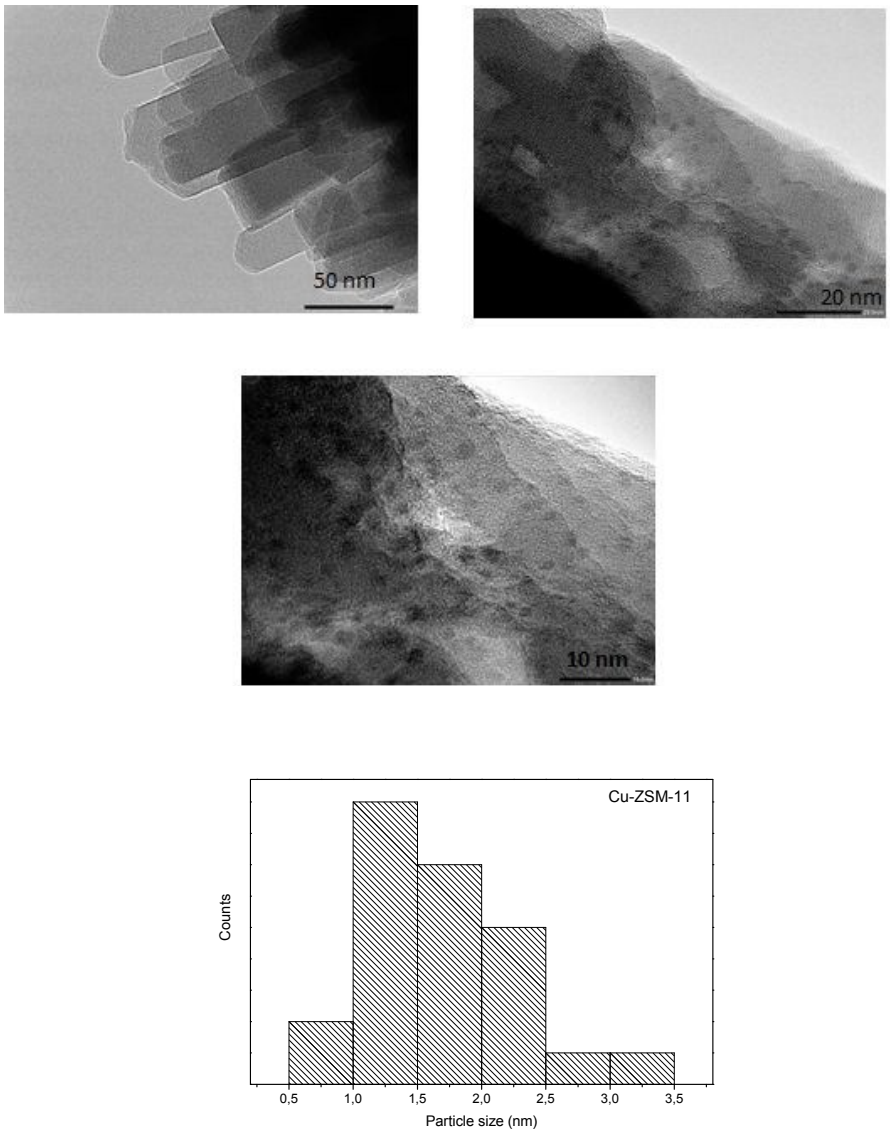

Figure 3. TEM images at different scales (top) and distribution of particle sizes (down) of Cu-ZSM-11 catalyst.

View Article Online
DOI: 10.1039/C9NJ04106K

TEM images and the particle sizes distribution of the Cr-ZSM-11 catalyst are shown in Figure 4. The images allow us to observe the dispersion of the metal particles on the surface of the crystals, as well as their small size when Cr was incorporated into the zeolite. Newly, the procedure described above was done to measure metal particles size from the TEM micrograph, by counting more than 50 particles in each case. It can be observed that Cr nanoparticles are less dispersed than Cu nanoparticles on the surface of the crystals. In addition, the formation of agglomerates of Cr nanoparticles was observed, this increasing their average size, which ranged from 1.6 nm to 5.0 nm, majority between 2-3 nm, with an average size of ≈3.5 nm, higher than the case of Cu nanoparticles incorporated on zeolite.

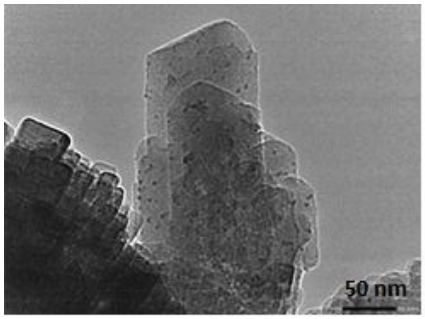

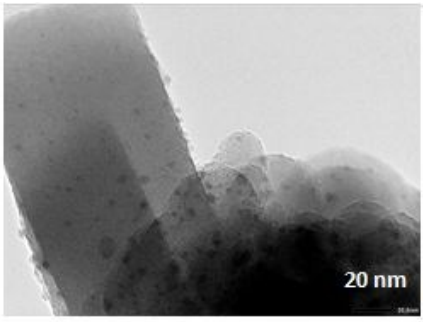

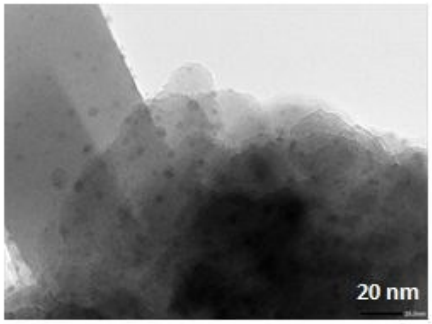

View Article Online
DOI: 10.1039/C9NJ04106K

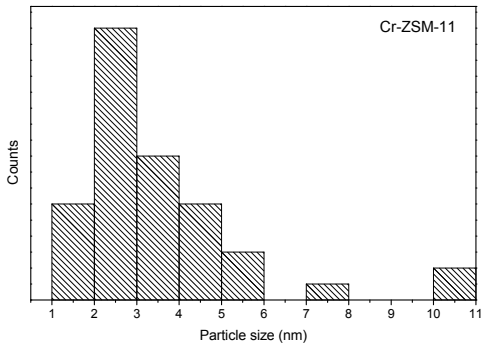

Figure 4. TEM images at different scales (top) and distribution of particle sizes (down) of Cr-ZSM-11 catalyst.

3.2. Catalytic Activity Results

The catalytic performances of the as-prepared zeolites were investigated in the selective oxidation of GLY performed in liquid phase and using aqueous H_2O_2 as oxidant. In these experiments, the effect of the operational parameters of reaction and the type of catalysts on the selective transformation of GLY to DHA and LA was analyzed. In all the cases, any organic solvent or additive was used.

The evolution of the GLY conversion and the selectivity to different products with reaction time for different catalysts are shown in Figure 5. Results were attained by employing 0.2 g of each catalyst, with a substrate/H_2O_2 molar ratio of 0.5, at 60 ºC and in the absence of solvent (see also Supporting Information Figure S3). A negligible GLY conversion of (~1 mol %) was detect in the absence of catalyst (data not shown). The reaction catalyzed by the H-ZSM-11 conventional zeolite without metal loading only gave a GLY conversion of 29.8 mol% at 4 h of reaction. The oxidation products detected in this case were GLA (20.6 mol %), GA (20.3 mol %) and FA (54.5 mol %). Interestingly, the GLY conversion increase notably when conventional ZSM-11 zeolites modified with copper and chromium are used, which indicates that the presence of these

View Article Online
DOI: 10.1039/C9NJ04106K

metals, and more importantly, the increase of Lewis acid sites in the solid catalysts could benefit such reaction.

In general, the zeolites with alkaline treatment resulted slightly more actives than the traditional ones, in terms of GLY conversion, at short reaction times (≤60-90 min of reaction). The lower Si/Al ratio in hierarchical zeolites (compared to starting zeolite) would be responsible for this behavior, and this could lead to a decrease in the strength of acid sites. For low Si/Al ratios in the framework of zeolites, the Brønsted /Lewis ratio generally decreases, which makes them more prone to deactivation in the early reaction stages, possibly due to the deposition of carbonaceous compounds within the pores of the zeolites. [18].

In the case of Cu-containing zeolites, Cu-ZSM-11 (T) hierarchical material was more active than Cu-ZSM-11 zeolite (until 120 min), when GLY conversion reaches a stationary plateau. This could be due to the lower ratio Brønsted/Lewis acid sites, resulting in a faster deactivation of them by blocking the pores with carbonaceous compounds.

In the case of Cr-zeolites, both Cr-ZSM-11 and Cr-ZSM-11 (T) catalysts lead to similar GLY conversion at shorter reaction times (< 60 - 90 min of reaction). Nevertheless, Cr-ZSM-11 offered higher GLY conversion than its analogous Cr-ZSM-11 (T) sample after this reaction time, which would also be related to the Brønsted/Lewis relationship of acid sites.

According to these data and considering the FTIR results above mentioned (see Figure 2), it is possible to adjudicate this behavior to the presence of Cr^{3+} species, since they can capture two electrons of atomic oxygen (valence shell structure from $3d^3$ to $3d^5$), thus promoting the activation of H_2O_2 and increasing the catalytic activity. Similar behavior

View Article Online
DOI: 10.1039/C9NJ04106K

was observed for Cu^{2+}, since it can easily get one electron from H_2O_2 to complete its valence shell structure $(3d^{10})^{26}$.

Commonly, the three types of reactions are involved during the oxidation of GLY dehydrogenation/hydrogenation reactions, C-O bond cleavage (dehydration) and C-C bond cleavage. Brønsted acid sites are crucial for dehydration of DHA/GLA (intermediates) to produce pyruvic aldehyde (not detected here) and then by rearrangement it generates LA, while Lewis acid sites catalyze hydrogenation and C-C cleavage of molecules producing compounds of lower number of carbon (C_2 and C_1), such as glycolic (GA), acetic (AA) and formic acid (FA) [4].

With respect to the products distribution, the main products detected during the GLY oxidation reaction employing Cu and Cr-Zeolites under the reaction conditions used herein were dihydroxyacetone (DHA), glyceraldehyde (GLA), glycolic acid (GA), lactic acid (LA), acetic acid (AA), and formic acid (FA), as well as other by-products (quantified but not identified). The GLY conversion and the products distribution determined over the time for Cu- and Cr-zeolites during the GLY oxidation are shown in Figure 5.

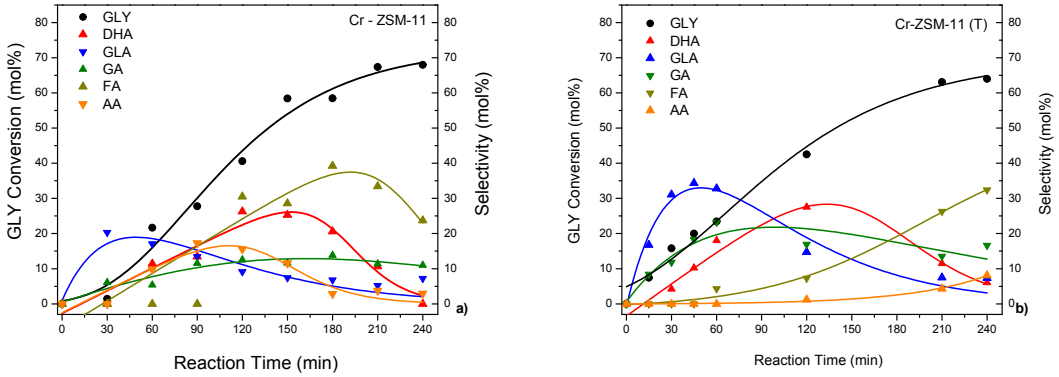

View Article Online
DOI: 10.1039/C9NJ04106K

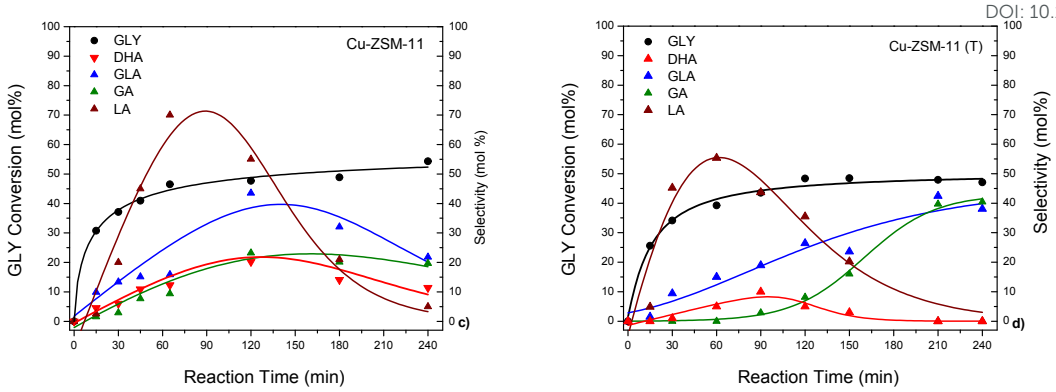

Figure 5. GLY conversion and selectivity (mol%) towards different products employing Metal-Zeolites. a) Cr-ZSM-11; b) Cr-ZSM-11(T); c) Cu-ZSM-11 and d) Cu-ZSM-11 (T).

As can be seen, glyceraldehyde (GLA) is one of the primary products formed at the beginning of the reaction, together with dihydroxyacetone (DHA), and also glycolic acid (GA, secondary product) when Cr-zeolites are employed (see reaction network S4 in the Supporting Information). The production of DHA reaches a maximum for Cr-ZSM-11 and Cr-ZSM-11 (T) around 120 min of reaction, then it continues being oxidized, so that over-oxidation products (mainly AA and FA) appear in the final reaction mixture. Interestingly, the appereance of the over-oxidation products is rather delayed in Cr-ZSM-11 (T) catalyst compared to Cr-ZSM-11 sample.This could be attributed to the higher content of Lewis acid sites present in the Cr-ZSM-11 sample that would be responsible to the formation of products generated by over-oxidation.

A different catalytic behavior is observed when employing Cu-ZSM-11 and Cu-ZSM-11 (T), where the main product of the reaction is the lactic acid (LA). In both cases, LA is generated at the beginning of the reaction together with GLA and DHA, and also GA, the two latter being formed in quite low amounts. The maximun production of LA is obtained at 60 min of reaction for both Cu-modified zeolites. Then, lactic acid is transformed into acetic and formic acids after 4 hours of reaction. In fact, the production of LA after 1 h of reaction was ~70 mol% (36% yield) when employing Cu-ZSM-11, that was higher

than LA selectivity (56.5 mol%, ~20% yield) obtained with Cu-ZSM-11 (T), always working under the same reaction conditions above-mentioned. This performance was in concordance with data published in the literature [27,28].

Moreover, another effect like "the confinement effect" in the microporous zeolites can be considered in these cases. This effect was corroborated by using zeolites with larger pore size, such as Cu-Beta, Cu-Y and Cu-MCM-41 that gave very low results in terms of glycerol conversion, reaching no more than 30% mol of GLY conversion at same reaction conditions, without detecting any product of interest (DHA or LA) [29].

Table 2 summarizes the selectivity to the more desired products DHA and LA at 60 and 120 min, since the majority generation of both products takes place at low reaction times. Indeed, it can be observed that DHA and LA selectivity values are low at the end of the reaction; this is mainly due to the continuous oxidation of these products into others such as acetic and formic acids as above-mentioned (see Figure 3). In subsequent studies, we decided to focus on DHA and LA since they have a higher commercial value than the rest of the products.

Table 2. GLY conversion and selectivity (mol %) towards DHA and LA over different Metal-Zeolites

Catalyst	Reaction Time (min)	GLY Conversion (mol%)	DHA Selectivity (mol%)	LA Selectivity (mol%)
Cr-ZSM-11	60	13.7	11.4	--
	120	40.6	28.3	--
Cr-ZSM-11 (T)	60	23.8	18.0	10.2
	120	42.5	27.5	5.3
Cu-ZSM-11	60	27.1	19.3	68.0
	120	42.5	25.2	49.0
Cu-ZSM-11 (T)	60	24.1	3,0	51.4
	120	31.5	5,0	41.5

Reaction conditions: Sol. GLY 0.5 M, GLY/H_2O_2 0.5 (mol/mol), T = 60°C, reaction time = 60, 120 min.

Considering the results exposed here, Cr-ZSM-11 showed the best catalytic behavior for the conversion of GLY to DHA, while Cu-ZSM-11 showed the major yields to LA,

respectively. Thus, these two zeolites were chosen to study the production of DHA or LA by optimizing different reaction parameters.

3.2.1 Selective production of DHA over Cr-zeolites

Figure 4 shows the change in the GLY conversion and DHA selectivity at 120 min of reaction time over Cr-ZSM-11 zeolite by analyzing the influence of different reaction parameters, such as tempertaure, amount of catalyst, and GLY/H_2O_2 molar ratio, this allowing elucidating the optimal reaction conditions to maximize DHA yields.

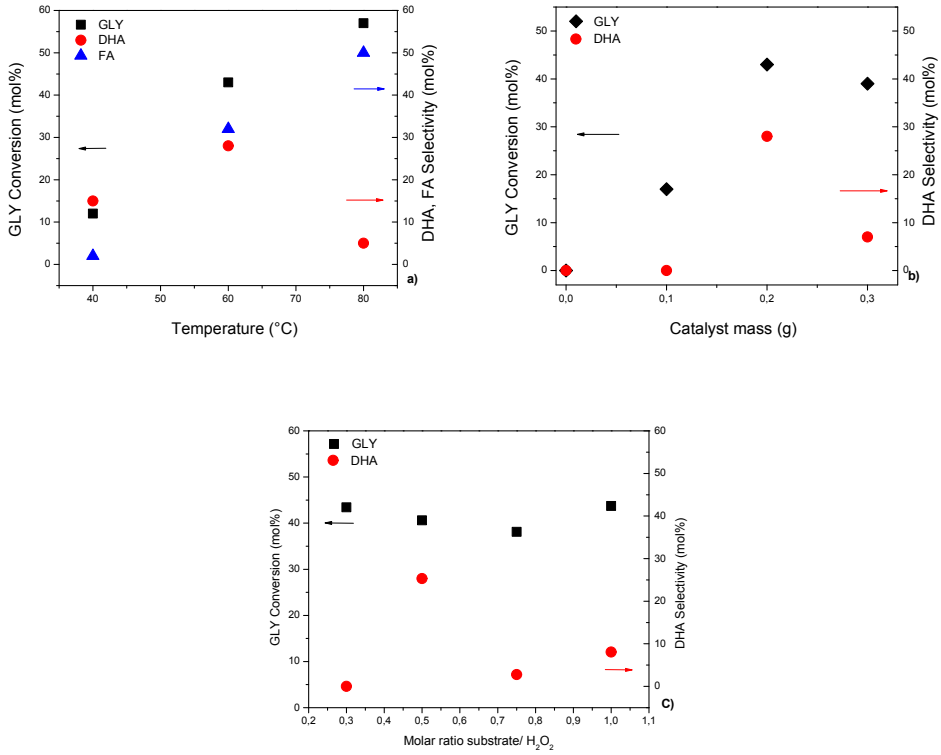

Figure 6. Influence of the reaction parameters on conversion and selectivity using Cr-ZSM-11 zeolite, at 120 min of reaction time: **a)** temperature; **b)** amount of catalyst; **c)** GLY/H_2O_2 molar ratio.

The effect of reaction temperature on catalytic activity of Cr -ZSM-11 for the conversion of GLY and selectivity to DHA was studied by varying this parameter from 40 to 80 °C (Figure 6a). In these experiments, GLY (0.5 M), H_2O_2 (30 %v/v), and mass of catalyst (0.2 g) were kept constant. With the increase of the reaction temperature, the GLY

conversion increased from <15% until 60%, as expected. However, excessive temperature (>60 ºC) exhibited an adverse effect on DHA selectivity, indicating the presence of over-oxidation process. This behavior is evidenced by the increase in the selectivity of FA [13, 30].

Catalyst mass introduced in the reaction was varied from 0.1 to 0.3 g by keeping the rest of operational parameters unchanged, and the results are given in Figure 6b. GLY conversion and DHA selectivity values increase together until catalyst mass of 0.2 g, where a maximum is achieved in both cases (GLY conversion ≈40%, and DHA selectivity ≈30%, respectively). Then, a slight decrease could be observed at higher amount of catalyst. This tendendy may be is related to an auto decomposition of hydrogen peroxide that gives water and oxygen as products ($H_2O_2 \rightarrow H_2O + ½ O_2$)[31], thus reducing GLY oxidation. This indicates that excessive amount of catalyst was unfavorable to the selective oxidation reaction of GLY to DHA. So, since DHA selectivity were considerably higher with 0.2g of catalyst, attempts to optimize reaction conditions were done employing this amount of catalyst.

As can be observed in Figure 4.c, the use of different concentrations of H_2O_2 (GLY/H_2O_2 molar ratios from 0.3 to 1.0) as oxidant generates a maximum DHA selectivity of ~28% at 2 h of reaction. The increase in the molar concentration of hydrogen peroxide produces not significantly changes in GLY conversion at 2 h, obtaining the best compromise between GLY conversion and DHA selectivity with substrate/H_2O_2 molar ratio of 0.5. Interestingly, it could be observed that working with higher concentration of hydrogen peroxide (substrate/H_2O_2 molar ratio = 0.3) a selectivity to DHA of ≈24 mol% was reached 15 min after the reaction has started, although this DHA production is strongly diminished at higher reaction times due to the favored over-oxidation processes taking place at higher oxidant concentrations.

To study the consumption of H_2O_2 due to the Cr-based catalyst loading the GLY oxidation was tested by slowly addition of the oxidant agent (at the beginning, at 60 min and at 120 min of reaction). It was observed that GLY conversion is mantained at ~70% after 240 min, while DHA selectivity increases up to 43% after 30 min of reaction (see supponting information S5). In addition, the fast appearance of formic acid (FA) could also be observed in this case from the beginning of the reaction, reaching 50% of FA selectivity at the end of the process (240 min of reaction).

Summarizing, it is possible to achieve ≈30% of DHA selectivity at ≈40% of GLY conversion by working at 60 ºC with 0.2 g of Cr-ZSM-11 catalyst and a GLY/H_2O_2 molar ratio of 0.5. The slowly addition of H_2O_2 in the reaction system allows increasing the DHA selectivity up to 43% at 30 min of reaction by keeping GLY conversion at adequate level.

3.2.2 Selective production of LA over Cu-zeolites

A study of main reaction parameters similar to that performed with Cr-ZSM-11 was carried out to analyze and maximize the conversion of GLY and the selectivity to LA when using Cu-ZSM-11 as catalyst (Figure 7). In this case, the conversion of GLY increases by increasing the reaction temperature from 40 to 80 °C, while the selectivity to LA remains close to 60%. Nevertheless, FA begins to be produced at 60-80 ºC, due to the over-oxidation reactions occurring at higher temperatures than 60° C (Figure 7a).

On the other hand, a similar behavior in terms of desired product selectivity was observed for Cu-ZSM-11 catalyst compared to Cr-ZSM-11 when analyzing the influence of the catalyst mass (Figure 7b). The conversion of GLY remains constant independently of the mass of catalyst used; while the selectivity to LA reaches a maximum when 0.2 g of catalyst is used, and then decreases with higher catalyst`s content.

View Article Online
DOI: 10.1039/C9NJ04106K

In the case of varying GLY/H_2O_2 molar ratio, a maximum in LA selectivity (close to 70%) is achieved over Cu-ZSM-11 catalyst with a substrate/H_2O_2 molar ratio of 0.5 at 60 min of reaction, when working at GLY conversion around 33% (Figure 7c).

As can be seen in the reported results, copper plays a fundamental role in the selective transformation of GLY towards LA. The best values of LA selectivity (~70 mol%) here attained with Cu-ZSM-11 catalyst at 60 min of reaction are superior to those reported in literature for other copper-based materials [17].

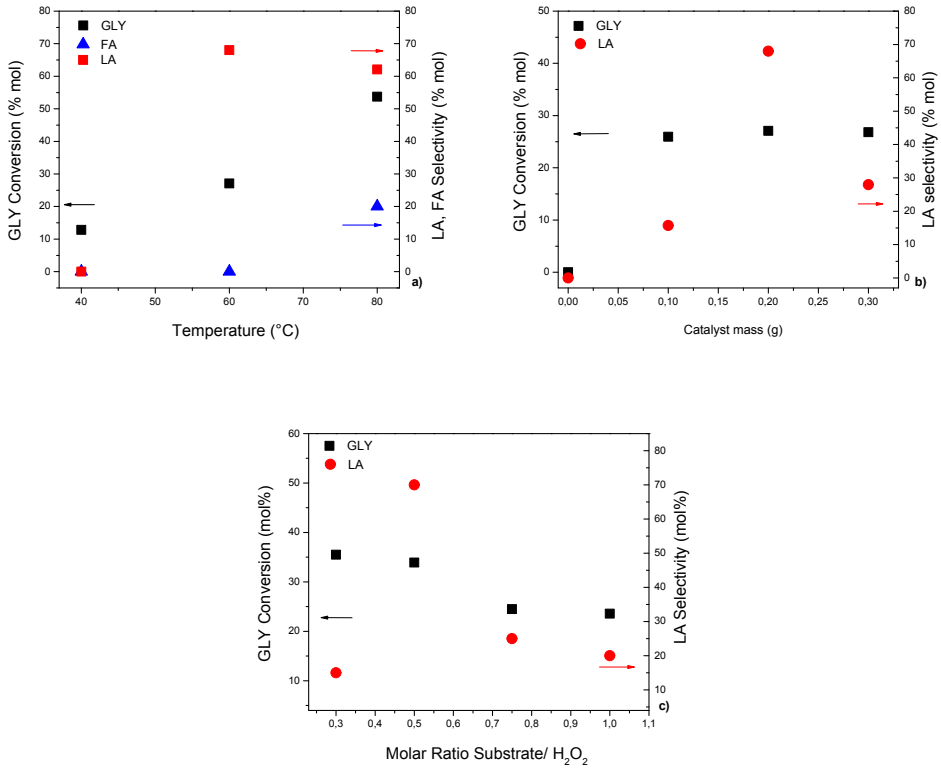

Figure 7. Influence of the reaction parameters on conversion and selectivity using Cu-ZSM-11 zeolite, at 60 min of reaction time: **a)** temperature; **b)** amount of catalyst; **c)** GLY/H_2O_2 molar ratio.

In order to evaluate the level of profitance of the oxidating agent in the catalytic process by using different metal-based zeolites, the efficiency of H_2O_2 was calculated by iodometric titration (see Experimental section).

For GLY oxidation employing Cu-ZSM-11 as catalyst, the calculated H_2O_2 efficiency was 22.5%, while by employing Cr-ZSM-11 as catalyst the oxidant eficiency was higher reaching 80.4%. These results are in agreement with catalytic activity (mol% GLY Conversion) previously mentioned with theses materials.

3.5 Reusability of the Cr-ZSM-11 and Cu-ZSM-11 catalyst

The possibility of reusing the heterogeneous catalysts is another key aspect for evaluating their catalytic performance. In this sense, the recyclability of Cr-ZSM-11 and Cu-ZSM-11 in the GLY oxidation with aqueous solution of H_2O_2 as oxidant was evaluated by performing several re-uses of the catalysts; the latter were recovered from the reaction mixture, and then used in a new experiment without any regeneration (see Experimental section).

As can be seen in Figure 8a, a partial decrease in the conversion of GLY can be observed after using five consecutive times the Cr-ZSM-11 zeolite under the same reaction conditions afore-mentioned. Thus, GLY conversion was ~70% by employing fresh catalyst, while a second use of the catalyst diminished GLY conversion to close to 53%. Then, in the third, fourth and fifth consecutive uses of the catalyst glycerol conversion remained practically constant at 48%. It is worth noting that these results were obtained without any regeneration treatment (for example, heat-treatment as calcination) all along the consecutive re-uses. Simultaneously, the selectivity to DHA (measured at 120 min) diminished from ~28% to ~13% after five catalytic cycles.

All these data clearly indicate that zeolite Cr-ZSM-11 is still active after five re-uses in the GLY oxidation reaction under mild conditions used herein. The slightly drop on GLY oxidation and DHA selectivity might be related to the increase of carbonaceous compounds adsorption onto the external surface of the solid catalyst (and also onto the internal channels), this making difficult the accessing of reactants to the active sites. In

addition, the active sites can be deactivated due to the presence of these carbonaceous molecules that do not diffuse towards the surface, and then to the liquid reaction mixture. To confirm these facts, structural (by XRD measurements) and acid (by FTIR spectroscopy with absorbed pyridine) properties of the used catalyst were determined.

By FTIR analysis, the B/L acid sites ratio for the Cr-ZSM-11 catalyst diminished from 2.96 to 2.73 μmol of pyridine/g of catalyst after the first cycle, this implicating a relative reduction of the acidity of only ~8%. After that, the B/L acid sites ratio remained unalterable after five uses, this meaning that the acid properties of the Cr-based catalyst are practically unchanged during reuses (see Supporting Information S6). In addition, no loss of crystallinity was observed in the used Cr-ZSM-11 zeolite with respect to the fresh catalyst (XRD patterns shown in Supporting Information S7) after five cycles of reaction. These evidences allow inferring that the Cr-ZSM-11 catalyst preserved its zeolitic structure and maintained a relative stable catalytic behavior during five reaction cycles.

In addition, the chromium content in the catalyst after the consecutive re-uses determined by ICP measurements was 2.71wt%, only slightly minor to the content of the fresh material (2.90wt%, see Table 1). From this result, it can be inferred that no leaching of the metal has taken place during reaction.

In summary, the reported results indicate that the Cr-ZSM-11 zeolite had long durability and was relatively resistent to catalytic deactivation. These results were similar to some reported results in literature [32] [33], where the incorporation of chromium into the zeolite catalysts increased not only its catalytic activity but also its thermal stability.

View Article Online
DOI: 10.1039/C9NJ04106K

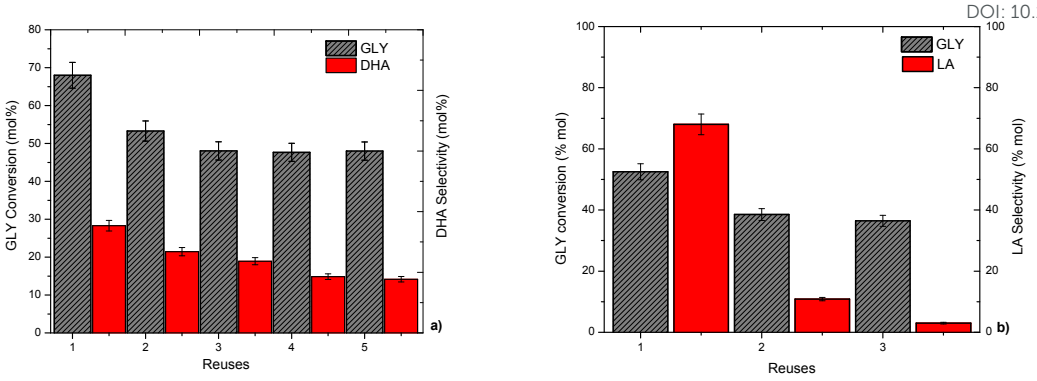

Figure 8. Reusability of Cr-ZSM-11(a) and Cu-ZSM-11 (b). Reaction conditions: GLY (0.5 M), H_2O_2 (30% v/v), catalyst 0.2 g, at 60 °C, 4 h duration of each cycle.

In the case of Cu-ZSM-11 (Figure 8b), the GLY conversion attained at the end of the first cycle was ~50% whereas a slight decrease (~38%) is observed for the second cycle; after that the GLY conversion remained constant in the third catalytic use. On the contrary,the LA selectivity was drastically decreased from 68 to 3% from the first to the third catalytic cycle, which means a decrease of more than 95% in LA selectivity. This behavior could be related to the strong decrease of both Lewis and Brønsted acid sites observed when studying the Cu-ZSM-11 used catalyst (after three reaction cycles) by means of FTIR spectroscopy with adsorbed pyridine. Indeed, the L/B acid sites ratio decreased from 1.55 µmol of pyridine/g of catalyst for the fresh sample to 0.78 in the case of the used catalyst (see Supporting Information S8).

On the other hand, the UV–vis–DRS spectroscopy is known to be a very sensitive probe for the identification and characterization of metal ion coordination and its existence in framework and/or in extra-framework position of metal containing zeolites. A major aspect that should be taken into account is the modifications induced in the structure of the catalytic sites due to the interaction with the reaction medium (see Supporting Information S9)

To evaluate that, the Cu-ZSM-11 catalyst used for three cycles has been calcined and used in a new oxidation reaction, under the same conditions. The GLY conversion achieved (47.8%) were very close to those obtained with the fresh catalyst (50%). This would confirm our hypothesis about the deposition of carbonaceous compounds in the catalyst during the catalytic cycle.

In addition, ICP measurements of the used catalyst sample allow determining a small decrease (≈ 20wt %) of the copper metal content copper with respect to the fresh material.

4. Conclusions

Microporous zeolite ZSM-11 was synthetized and modified by alkali treatment to generate mesoporosity (ZSM-11 (T)), achieving higher percentages of crystallinity and purity. Then, these catalytic materials were modified by the incorporation of transition metals (Cu and Cr) employing wet impregnation at 80° C, in rotatory evaporator. The textural and physicochemical properties was studied and analyzed in this work, using different characterization techniques as XRD, FTIR, TEM, N_2 sorption isotherms, ICP, TPR, among others. These catalysts showed a great potential for the conversion of GLY to produce DHA and LA employing H_2O_2 as an oxidant and mild reaction conditions.

The reaction catalyzed by H-ZSM-11 without metal loading only gives a 29.8% of GLY conversion at 4 h of reaction without production of products of interest, such as DHA or LA. Instead, the GLY conversion increased notably by employing copper and chromium modified zeolites, due to the modification of its acid properties (Brønsted/Lewis ratio). Although all the Metal-ZSM-11 modified samples studied had a similar metal content (~3 wt %), the Cr-ZSM-11 was more active than the other catalysts giving ~70% of GLY conversion with a maximum DHA selectivity of ~28% at 120 min of reaction. On the other hand, Cu-ZSM-11 catalyst resulted more selective towards the LA formation, reaching 68% of LA selectivity with a GLY conversion of 55% at 60 min of reaction.

Main reaction parameters were studied by using both catalysts in order to obtain the optimal reaction conditions to accurate the maximum yields of both DHA (with Cr-ZSM-11) and LA (with Cu-ZSM-11). The optimal reaction conditions were quite similar for both Cr- and Cu-based materials. Thus, the selected temperature for maximizing DHA and LA production during GLY oxidation with aqueous H_2O_2 over Cr-ZSM-11 and Cu-ZSM-11 catalyst, respectively was 60 ºC. The optimum GLY/H_2O_2 molar ratio was 0.5, while the optimum mass of catalyst employed was 0.2 g.

The recyclability of Cr-ZSM-11 and Cu-ZSM-11 was evaluated by performing several re-uses of the catalysts. In these cases, the solids were recovered from the reaction mixture, and then used as catalysts in a new experiment without any regeneration.

In the case of Cr-ZSM-11 catalyst, a slightly decrease in the conversion of glycerol can be observed after five cycles. Thus, GLY conversion was ~70% by employing fresh catalyst, while in a second use it diminished to close to 53%. Then, the GLY conversion remained practically constant at 48% in the followed consecutive re-uses. DHA selectivity also suffered variation from 28% to 18% between the first and second reuses, respectively, then remaining constant at 13% in third, fourth and fifth consecutive uses. Cr-ZSM-11 zeolite demonstrated a long durability and relatively high resistance to catalytic deactivation, in the GLY oxidation reaction under the mild reaction conditions here employed. This fact is mainly due to the maintainance of structural and acid properties of the solid catalyts after recycling. These results confirm some literature reports where the incorporation of Cr into the zeolites increased both catalytic activity and thermal stability. On the other hand, Cu-ZSM-11 catalyst was studied during three consecutive cycles without any regeneration treatment. GLY conversion was ~55% when employing fresh catalyst, decreasing until 38% in the second use, and then remaining constant in third use. Nevertheless, the excellent selectivity to LA initially observed

suffered a strong diminution from 68% to 3% by going from the first to the third cycle. This catalytic behavior for Cu-ZSM-11 catalyst indicated that Cu-based zeolite suffered a decrease in both GLY conversion and mainly LA selectivity with reuses, possibly due to the high deposition of carbonaceous compounds onto the surface and into the zeolitic pores of the catalyst, thus blocking both their acid sites and channels. Taking into consideration that the recycling tests were made without regeneration, is possible to overcome Cu-ZSM-11 deactivation by performing thermal regeneration of the catalyst between the catalytic cycles.

Further studies are actually carrying out in our research group to improve this research.

5. Acknowledgements

This project was partially supported by CONICET PIP 112 201301 00146 CO and PID-UTN3493. We would also wish to thank CONICET and UTN.

References

1 G. W. Huber, S. Iborra and A. Corma, 2006, **2**, 4044–4098.

2 Direccion de Bioenergia Argentina. Camara Argentina de Biocombustibles, .

3 S. S. Yazdani and R. Gonzalez, *Current Opinion in Biotechnology*, 2007, **18**, 213–219.

4 D. Kubiĉka, I. Kubiĉkov́ and J. Ĉejka, *Catalysis Reviews - Science and Engineering*, 2013, **55**, 1–78.

5 B. Katryniok, H. Kimura, E. Skrzyńska, J.-S. Girardon, P. Fongarland, M. Capron, R. Ducoulombier, N. Mimura, S. Paul and F. Dumeignil, *Green Chemistry*, 2011, **13**, 1960–1979.

6 F. Jørôme and Y. Pouilloux, *ChemSusChem*, 2008, **1**, 586–613.

7 T. Stanko, L. Tietze and E. Arch, *American Journal of Clinical Nutrition*, 1992, **56**, 630–635.

8 R. B. Æ. N. Katsikis and Æ. S. V. Æ. D. Hekmat, *Bioprocess and Biosystems Engineering*, 2005, **28**, 37–43.

9 J. Svitel and E. Sturdik, *Journal of Fermentation and Bioengineering*, 1994, **1783**, 351–355.

10 N. Dimitratos, F. Porta and L. Prati, *Applied Catalysis A: General*, 2005, **291**, 210–214.

11 J. Lin, J. Chen, C. Hsiao, Y. Kang and B. Wan, *Applied Catalysis B: Environmental*, 2002, **36**, 19–29.

12 X. Wang, C. Shang, G. Wu, X. Liu and H. Liu, *Catalysts*, 2016, **6**, 101.

13 W. Hu, D. Knight, B. Lowry and A. Varma, *Industrial and Engineering Chemistry Research*, 2010, **49**, 10876–10882.

14 C. Crotti and E. Farnetti, *Journal of Molecular Catalysis A: Chemical*, 2015, **396**, 353–359.

15 F. Andres, C. Martinez, E. Marcos, M. Dom and R. P. De Souza, *Trends in Food Science and Technology*, 2013, **30**, 70–83.

16 Y. Li, S. Chen, J. Xu, H. Zhang, Y. Zhao, Y. Wang, Z. Liu, M. Sciences and M. Sciences, *Clean - Soil, Air, Water*, 2014, **42**, 1140–1144.

17 C. Zhang, T. Wang, X. Liu and Y. Ding, *Journal of Molecular Catalysis A: Chemical*, 2016, **424**, 91–97.

18 J. Přech, P. Pizarro, D. P. Serrano and J. Áejka, *Chemical Society Reviews*, 2018, **47**, 8263–8306.

19 G. T. Kokotailo, P. Chu, S. L. Lawton and W. M. Meier, *Nature*, 1978, 275, 119–120.

20 H. Liu, S. Liu, S. Xie, C. Song and W. Xin, *Catalysis Letters*, 2015, **145**, 1972–1983.

21 L. B. Pierella, G. A. Eimer and O. A. Anunziata, *Reaction Kinetics and Catalysis Letters*, 1998, **63**, 271–278.

22 C. A. Emeis, *Journal of Catalysis*, 1993, 141, 347–354.

23 J. C. Groen, L. A. A. Peffer and J. Pérez-Ramírez, *Microporous and Mesoporous*

Materials, 2003, **60**, 1–17.

24 L. B. Pierella, C. Saux and S. C. Caglieri, *Applied Catalysis A: General*, 2008, **347**, 55–61.

25 J. C. Groen, J. A. Moulijn and J. Pe, *Microporous and Mesoporous Materials 87*, 2005, **87**, 153–161.

26 J. Luo, H. G. Li, N. Zhao, F. Wang and F. K. Xiao, *Ranliao Huaxue Xuebao/Journal of Fuel Chemistry and Technology*, 2015, **43**, 677–683.

27 A. B. F. Moreira, A. M. Bruno, M. M. V. M. Souza and R. L. Manfro, *Fuel Processing Technology*, 2016, **144**, 170–180.

28 D. Roy, B. Subramaniam and R. V. Chaudhari, *ACS Catalysis*, 2011, **1**, 548–551.

29 G. Sastre and A. Corma, *Journal of Molecular Catalysis A: Chemical*, 2009, **305**, 3–7.

30 C. Crotti and E. Farnetti, *Journal of Molecular Catalysis A: Chemical*, 2015, 353–359.

31 V. R. Choudhary, N. S. Patil, N. K. Chaudhari and S. K. Bhargava, *Journal of Molecular Catalysis A: Chemical*, 2005, **227**, 217–222.

32 C. Saux and L. B. Pierella, *Applied Catalysis A: General*, 2011, **400**, 117–121.

33 P. H. Hoang, N. T. Nhung and L. Q. Dien, *AIP Advances*, 2017, 7, 1-11.

View Article Online
DOI: 10.1039/C9NJ04106K

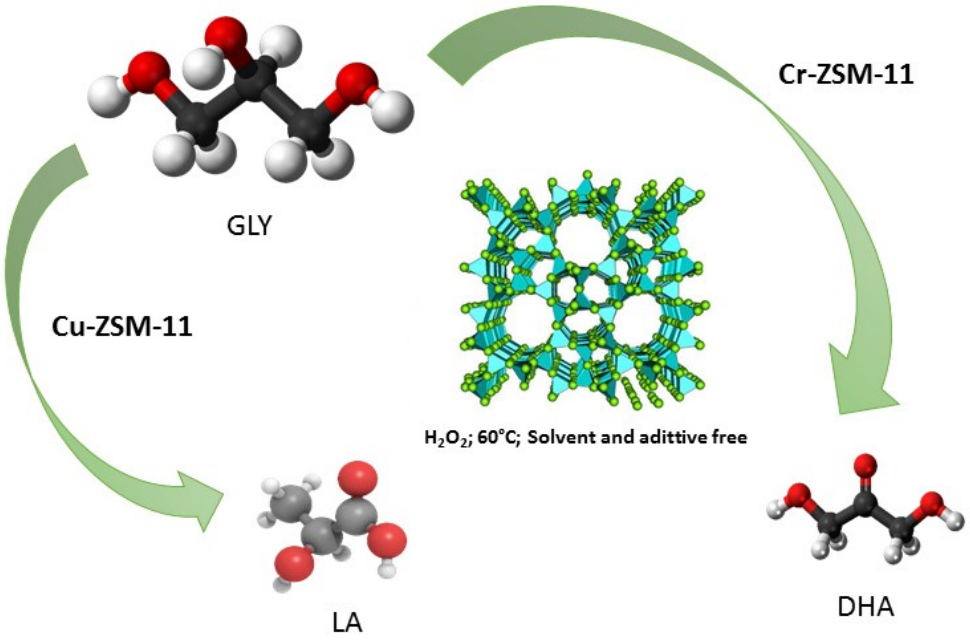

Selective oxidation of glycerol towards dihidroxyacetone and lactic acid, employing micro/mesoporous zeolites with Copper (II) and Chromium (III).

199x162mm (96 x 96 DPI)